MATERIALS PHYSICS AND MECHANICS RESEARCH ARTICLE

**Submitted: October 29, 2025** **Revised: November 18, 2025** **Accepted: December 03, 2025**

# Band gap engineering with strains induced by quantum dots in semiconductors nanowires

**Nguyen Van Tuyen [1,2], A.L. Kolesnikova [1,3], M.Yu. Gutkin [1,3,4], A.E. Romanov [1,5,6]** ✉

[1] ITMO University, St. Petersburg, Russia

[2] Sao Do University, Hai Phong City, Vietnam

[3] Institute for Problems in Mechanical Engineering, Russian Academy of Sciences, St. Petersburg, Russia

[4] Peter the Great St. Petersburg Polytechnic University, St. Petersburg, Russia

[5] Ioffe Institute, Russian Academy of Sciences, St. Petersburg, Russia

[6] Togliatti State University, Togliatti, Russia

✉ aeromanov@itmo.ru

**ABSTRACT**

This work examines the influence of quantum dots embedded in semiconductor nanowires with lattice parameters different from those of the surrounding nanowire material on the nanowire band gap. Using the found analytical formulas for the elastic fields of cylindrical, hemispherical, and conical inclusions simulating quantum dots and located along the nanowire symmetry axis, the maps of the elastic dilations are depicted and the regions of their extremes near the nanowire surface are identified. Calculations are performed within the framework of the isotropic linear theory of elasticity. For GaN nanowires containing axisymmetric quantum dots of varying shapes and compositions, the deformation potentials and corresponding changes in the band gap in the nanowire regions of elastic dilation extremes are calculated. The dependence of local change in the band gap in GaN nanowires on the lattice mismatch parameter between the quantum dots and NWs are presented. It is shown that the semiconductor nanowire band structure depends on the quantum dot shape, material, and size, and the band gap of GaN nanowires can locally vary by approximately 10 % of its tabulated value. The response of the band gap of a semiconductor nanowire to the elastic field of quantum dot embedded in this wire allows one to nanowire band gap engineering by varying the parameters of the quantum dot.

**KEYWORDS**

semiconductor nanowire • quantum dot • elastic fields • deformation potential • band gap

**Funding.** *AK and MG are thankful to the Ministry of Education and Science of the Russian Federation for support under the state assignment No. 124041100008-5 for the Institute for Problems in Mechanical Engineering of the Russian Academy of Sciences.*

**Citation:** Nguyen Van Tuyen, Kolesnikova AL, Gutkin MYu, Romanov AE. Band gap engineering with strains induced by quantum dots in semiconductors nanowires. *Materials Physics and Mechanics*. 2025;53(5): 42–49. http://dx.doi.org/10.18149/MPM.5352025_3

## Introduction

With the development of modern science and technology, quantum dots are playing an increasingly important role in electronics, optoelectronics, photonics and other applications [1,2]. Quantum dots (QDs) are tiny semiconductor particles, typically ranging in size from 2 to 10 nanometers, possessing unique optical and electronic properties due to quantum mechanical effects [3–5]. The optical and electronic properties of QDs are determined by their size and shape, which allows for precise control of light emission and

absorption [6,7]. Crystalline QDs embedded in the matrix of another crystalline material possess an elastic field [8–10] depending on QD and matrix shape, material and size. This results in the emergence of a deformation potential in the QDs themselves and the surrounding matrix. This deformation potential influences the formation of the band structure of the QDs and the matrix [11–14]. QDs embedded in nanowires (NW) uniquely combine the tunable optical properties of QDs with the unique electronic and optoelectronic characteristics of the nanowires, enabling precise control of the quantum-optical behavior of the semiconductor wire heterostructure. This makes them highly promising for applications in quantum photonics, optoelectronics, and sensors [15–17]. As mentioned above, the strain induced by the presence of QDs in NW strongly affects the band structure of the nanowires. Detailed studies of the influence of QD strain on the band structure of nanowires can be found in a few papers [18–20].

In this paper, using our analytical calculations, we briefly analyze the elastic strain field of cylindrical, hemispherical, and conical QDs in nanowire. Then, in the framework of the **k·p** perturbation theory approach, we study the effect of QD induced strains on the electronic band gap of GaN nanowires.

## Elastic field of the quantum dot in the wire

The QD buried in material matrix can be modeled by an elastic dilatational inclusion (DI) with an eigenstrain ${}^{\mathrm{DI}}\varepsilon_{ii}^{*}$ due to the mismatch between the lattice constants of the QD and the surrounding crystal matrix:

$${}^{\mathrm{DI}}\varepsilon_{ii}^{*} = \varepsilon^{*}\delta(\Omega), \tag{1}$$

where $\delta(\Omega) = \begin{cases} 1, & \boldsymbol{r} \in \Omega \\ 0, & \boldsymbol{r} \notin \Omega \end{cases}$, $\Omega$ is the DI region. There is no summation of $i$ in ${}^{\mathrm{DI}}\varepsilon_{ii}^{*}$, $i$ is a coordinate in any orthogonal coordinate system.

In Eq. (1), misfit parameter $\varepsilon^{*}$ is found using the following relationship (see, for example, [21,22]):

$$\varepsilon^{*} = \frac{a_{QD} - a_m}{a_m}, \tag{2}$$

where $a_{QD}$ and $a_m$ are the lattice constants of QD and surrounding matrix in the absence of strains. For the crystal lattice parameters, $a$ and $c$ of wurtzite structure $In_xGa_{1-x}N$, Vegard's law is applied [23,24]:

$$a_{\mathrm{In}_x\mathrm{Ga}_{1-x}N} = x \cdot a_{\mathrm{InN}} + (1-x) \cdot a_{\mathrm{GaN}},\ c_{\mathrm{In}_x\mathrm{Ga}_{1-x}N} = x \cdot c_{\mathrm{InN}} + (1-x) \cdot c_{\mathrm{GaN}}. \tag{3a,b}$$

In our consideration, QDs are axially symmetric DIs of the cylinder, hemisphere and cone shapes (Fig. 1). To calculate the elastic fields of DIs in NW, we model DIs as a set of infinitesimally thin coaxial disks (DDs) of radius $c$ with eigenstrain ${}^{DD}\varepsilon_{ii}^{*}$ [25–27], uniformly distributed with a constant density $\rho$ along the axis of symmetry:

$${}^{\mathrm{DD}}\varepsilon_{ii}^{*} = bH\left(1 - \frac{r}{c}\right)\delta(z - z_0), \tag{4}$$

$${}^{\mathrm{DI}}\varepsilon_{ii}^{*} = \int_{z_1}^{z_2} {}^{\mathrm{DD}}\varepsilon_{ii}^{*}(r, z - z_0)\rho dz_0 = \int_{z_1}^{z_2} bH\left(1 - \frac{r}{c}\right)\delta(z - z_0)\rho dz_0 = \varepsilon^{*}\delta(\Omega), \tag{5}$$

where $b$ is a coefficient with the dimension of length, $H(\zeta) = \begin{cases} 1, \zeta > 0 \\ 0, \zeta < 0 \end{cases}$ is the Heaviside step function, $\delta(z)$ is the Dirac delta-function, $c$ is the radius of the disk, $z_0$ is the coordinate of disk, and $[z_1, z_2]$ is an extent of DI along the $z$-axis.

In this approach, the elastic fields of DIs are obtained by integrating the

corresponding components of the elastic fields of infinitesimal thin DDs in NW, found by us earlier [28,29].

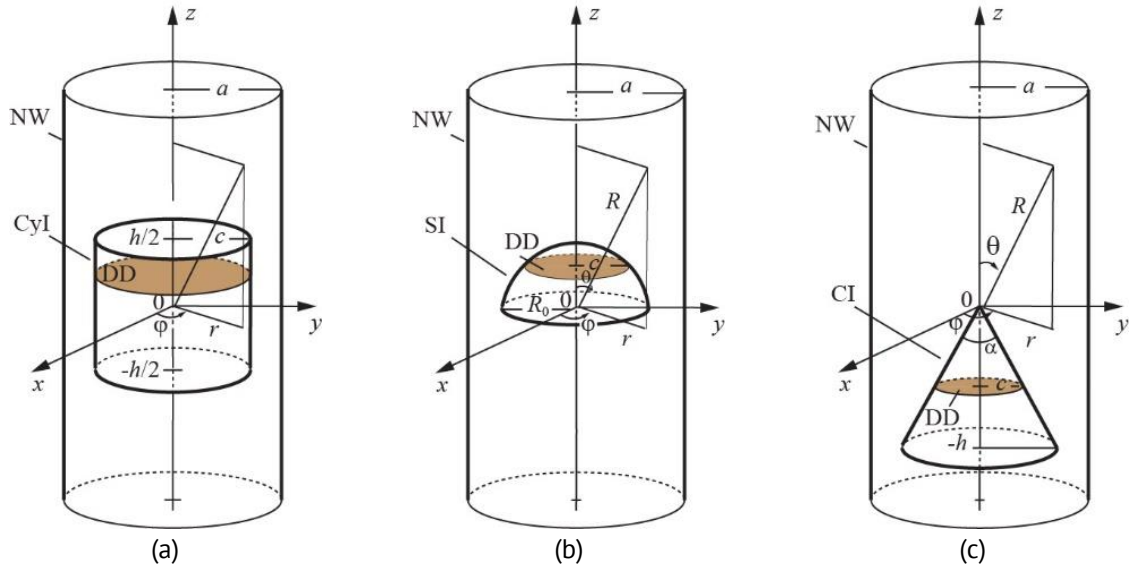


**Fig. 1**. Quantum dots modeled by the dilatational inclusions in the shape of a cylinder - CyI (a), a hemisphere - SI (b), and a cone - CI (c), embedded in a circular nanowire - NW. The cartesian $(x, y, z)$, cylindrical $(r, \varphi, z)$, and spherical $(R, \theta, \varphi)$ coordinate systems are shown. Dilatational disks – DDs, which are used to "assemble" the inclusions, are also depicted

The elastic fields (displacements ${}^{\mathrm{DI}}u_i$, strains ${}^{\mathrm{DI}}\varepsilon_{ij}$, and stresses ${}^{\mathrm{DI}}\sigma_{ij}$) of DI in NW include two parts: the first part corresponds to DI in infinite elastic space, the second part corresponds to the contribution of the free surface of NW, see [28,29] and [30], in which DD and DI have the same radius as NW.

For example, total displacements ${}^{\mathrm{DI}}u_i$ of DI are calculated by the following equation:

$${}^{\mathrm{DI}}u_i = \int_{z_1}^{z_2} {}^{\mathrm{DD}}u_i(r, z - z_0)\rho dz_0 = {}^{\infty\mathrm{DI}}u_i + {}^{\mathrm{imDI}}u_i. \quad (6)$$

where ${}^{\infty\mathrm{DI}}u_i$ and ${}^{\mathrm{imDI}}u_i$ are displacements of DI in an infinite elastic media and image part due to effect of free lateral surface of NW, respectively [28,29]. Note that all the fields found have an analytical representation in the form of integrals or series.

Based on Eq. (6), we can find elastic strains for axially symmetric DI by the following expressions in the cylindrical $(r, \varphi, z)$ and spherical $(R, \theta, \varphi)$ coordinate systems:

$${}^{\mathrm{DI}}\varepsilon_{rr} = \frac{\partial {}^{\mathrm{DI}}u_r}{\partial r} - \varepsilon^* \delta(\Omega),\ {}^{\mathrm{DI}}\varepsilon_{\varphi\varphi} = \frac{{}^{\mathrm{DI}}u_r}{r} - \varepsilon^* \delta(\Omega), \quad (7a,b)$$

$${}^{\mathrm{DI}}\varepsilon_{zz} = \frac{\partial {}^{\mathrm{DI}}u_z}{\partial z} - \varepsilon^* \delta(\Omega),\ {}^{\mathrm{DI}}\varepsilon_{rz} = \frac{1}{2}\left(\frac{\partial {}^{\mathrm{DI}}u_r}{\partial z} + \frac{\partial {}^{\mathrm{DI}}u_z}{\partial r}\right), \quad (7c,d)$$

$${}^{\mathrm{DI}}\varepsilon_{RR} = \frac{\partial {}^{\mathrm{DI}}u_R}{\partial R} - \varepsilon^* \delta(\Omega),\ {}^{\mathrm{DI}}\varepsilon_{\theta\theta} = \frac{1}{R}\frac{\partial {}^{\mathrm{DI}}u_\theta}{\partial \theta} + \frac{{}^{\mathrm{DI}}u_R}{R} - \varepsilon^* \delta(\Omega), \quad (8a,b)$$

$${}^{\mathrm{DI}}\varepsilon_{\varphi\varphi} = \frac{{}^{\mathrm{DI}}u_\theta}{R} cot\,\theta + \frac{{}^{\mathrm{DI}}u_R}{R} - \varepsilon^* \delta(\Omega),\ {}^{\mathrm{DI}}\varepsilon_{R\theta} = \frac{1}{2}\left(\frac{1}{R}\frac{\partial {}^{\mathrm{DI}}u_R}{\partial \theta} + \frac{\partial {}^{\mathrm{DI}}u_\theta}{\partial R} - \frac{{}^{\mathrm{DI}}u_\theta}{R}\right). \quad (8c,d)$$

The elastic hydrostatic strain of DI in NW is determined by following equation:

$${}^{\mathrm{DI}}\Delta = {}^{\mathrm{DI}}\varepsilon_{rr} + {}^{\mathrm{DI}}\varepsilon_{\varphi\varphi} + {}^{\mathrm{DI}}\varepsilon_{zz} = {}^{\mathrm{DI}}\varepsilon_{RR} + {}^{\mathrm{DI}}\varepsilon_{\theta\theta} + {}^{\mathrm{DI}}\varepsilon_{\varphi\varphi}. \quad (9)$$

From Eq. (9), we can depict the maps of the distribution of the elastic hydrostatic strains for considered QDs in NW as it is shown in Fig. 2.

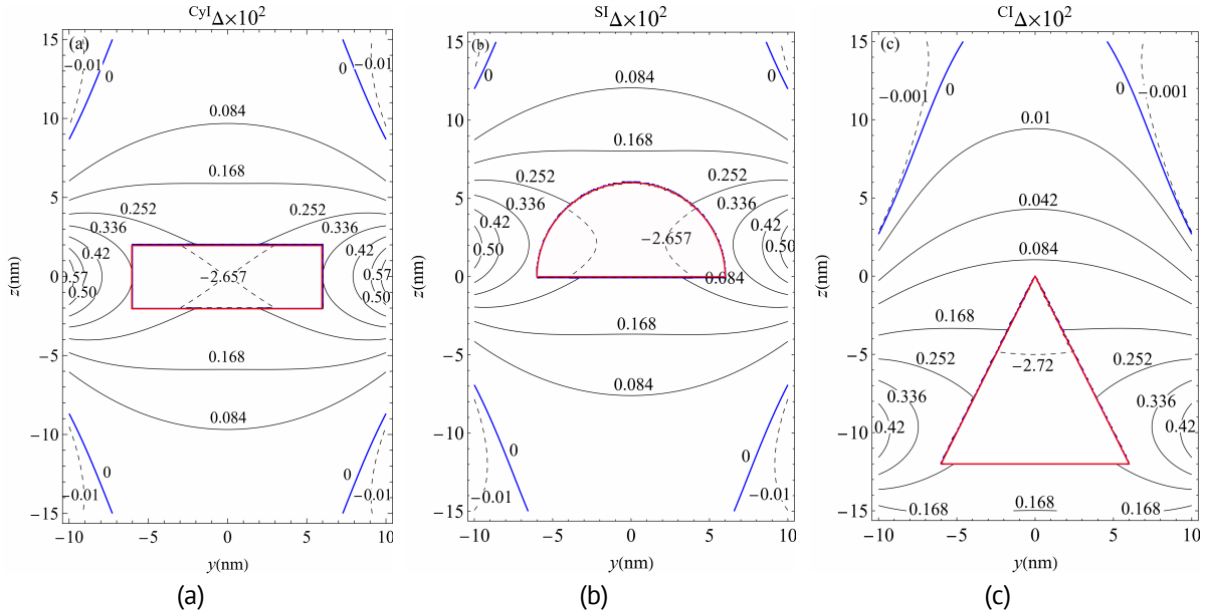


**Fig. 2**. The maps of elastic hydrostatic strains due to $In_{0.2}Ga_{0.8}N$ quantum dots (QDs) in GaN nanowire (NW): (a) cylindrical QD, (b) hemispherical QD, and (c) conical QD. The parameters for calculations: the volume of the base of QD $V = 144\pi$ nm$^3$; NW radius and the radius of QD base are 10 and 6 nm, respectively; the Poisson ratio of GaN $v = 0.234$ [22]; the misfit parameter of $In_{0.2}Ga_{0.8}N$ in GaN matrix is $\varepsilon^* = 0.021$

## Effect of the strain on the NW band gap

The influence of strain of QD on the band structure is evaluated using the **k·p** perturbation approach proposed by Bir and Pikus [11]. In unstrained wurtzite GaN, there are three closely spaced top valence bands (VB) at the center of the Brillouin zone, commonly referred to as heavy-hole (HH), light-hole (LH), and crystal-field split-off hole (CH) [14,31]. These VB states have atomic *p*-orbital character, in contrast to the bottom conduction band (CB), which has atomic *s*-orbital character. The presence of QDs in the material matrix creates a strain field, thereby changing the band structure of the material through the deformation potential. Since the large band gap of GaN reduces the interaction of CB and VB states, the Hamiltonian for the strain dependence of VB can be separately given by the 6 × 6 matrix [11]:

$$H^v(k,\varepsilon) = \begin{pmatrix} F & 0 & -H^* & 0 & K^* & 0 \\ 0 & G & \Delta & -H^* & 0 & K^* \\ -H & \Delta & \lambda & 0 & I^* & 0 \\ 0 & -H & 0 & \lambda & \Delta & I^* \\ K & 0 & I & \Delta & G & 0 \\ 0 & K & 0 & I & 0 & F \end{pmatrix}. \quad (10)$$

Here $\Delta = \sqrt{2}\Delta_3$, $F = \Delta_1 + \Delta_2 + \lambda + \theta$; $G = \Delta_1 - \Delta_2 + \lambda + \theta$, $K = A_5 k_+^2 + D_5\varepsilon_+$, $H = i(A_6 k_z k_+ + A_7 k_+ + D_6\varepsilon_{z+})$, $I = i(A_6 k_z k_+ - A_7 k_+ + D_6\varepsilon_{z+})$, $\lambda = A_1 k_z^2 + A_2 k_\perp^2 + +D_1\varepsilon_{zz} + D_2(\varepsilon_{xx} + \varepsilon_{yy})$, $\theta = A_3 k_z^2 + A_4 k_\perp^2 + D_3\varepsilon_{zz} + D_4(\varepsilon_{xx} + \varepsilon_{yy})$, $k_\pm = k_x \pm ik_y$, $k_\perp^2 = k_x^2 + k_y^2$, $k_\pm = k_x \pm ik_y$, $\varepsilon_{z\pm} = \varepsilon_{xz} \pm i\varepsilon_{yz}$, $\varepsilon_\pm = \varepsilon_{xx} - \varepsilon_{yy} \pm 2i\varepsilon_{xy}$, $\varepsilon_\perp = \varepsilon_{xx} + \varepsilon_{yy}$, where parameters $D_j$ ($j$ = 1–6) denote the deformation potentials VB, and $A_j$ ($j$ = 1 to 7) are equivalent to the Luttinger parameters [31], parameter $\Delta_1$ is the crystal-field parameter, while $\Delta_2$ and $\Delta_3$ are the spin-orbit energy parameters. The diagonalization of the matrix (10) yields the three distinct VB maxima $E_{v,j}$.

The edge of conduction band $E_c$ (due to strain) can be expressed as [14,32]:

$$E_c = \frac{\hbar^2 k_z^2}{2m_{e||}} + \frac{\hbar^2 (k_x^2 + k_y^2)}{2m_{e\perp}} + \alpha_{\parallel}\varepsilon_{zz} + \alpha_{\perp}(\varepsilon_{xx} + \varepsilon_{yy}), \quad (11)$$

where $k_x, k_y, k_z$ are components of wave vector on direction of the $x, y, z$ axes respectively; respect $\alpha_{\perp}$, $\alpha_{\parallel}$ and $m_{e\parallel}$,$m_{e\perp}$ denote the CB deformation potentials and electron effective mass, respectively. Here we only consider the ground energy state (**k** = 0), so Eqs. (10) and (11) are much simplified. The band structure parameters for wurtzite GaN are presented in Table 1.

**Table 1.** Band structure parameters for wurtzite GaN [33]

| Parameters | Values, eV | Parameters | Values, eV |
|---|---|---|---|
| $E_g$ | 3.479 | $D_1$ | - 41.4 |
| $D_{cr}$ | 0.010 | $D_2$ | - 33.3 |
| $D_{SO}$ | 0.015 | $D_3$ | 8.2 |
| $\Delta_1 = \Delta_{cr}$ | 0.022 | $D_4$ | - 4.1 |
| $\Delta_2 = \Delta_3 = \Delta_{SO}/3$ | 0.005 | $D_5$ | - 4.7 |
| $\alpha_{\|\|}$ | - 44.5 | $D_6$ | - 7.5 |
| $\alpha_{\perp}$ | - 44.5 | | |

The strains influence both valence and conduction bands via Eqs. (10) and (11), therefore the band gap of material changes due to the strains. The strong change of band gap is near the lateral surface of NW. The distribution of the change of band gap $\Delta E_g^{def}$ along lateral surface of NW is shown in Fig. 3.

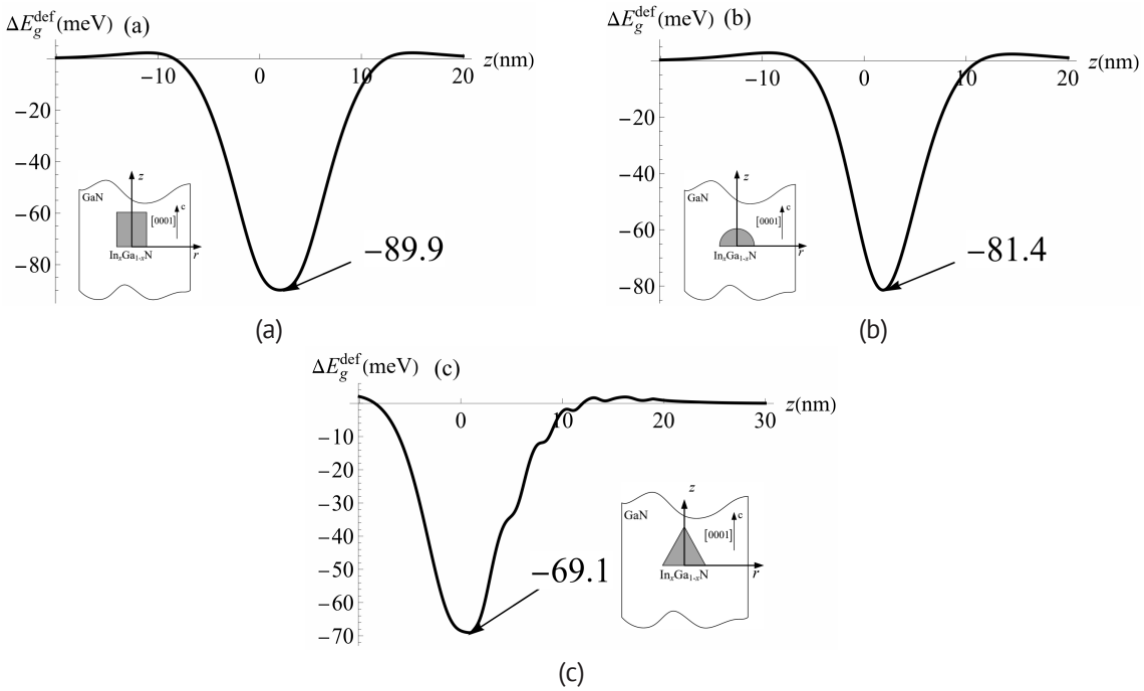


**Fig. 3**. The distribution of the change of the band gap $\Delta E_g^{\mathrm{def}}$ of GaN nanowire (NW) due to the presence of the $In_{0.2}Ga_{0.8}N$ quantum dot (QD), along free surface of NW. (a) cylindrical QD, (b) hemispherical QD, and (c) conical QD. The parameters for calculations: the volume of the base of QD $V = 144\pi$ nm$^3$; NW radius and the radius of QD base are 10 nm and 6 nm, respectively; the Poisson ratio of GaN $v = 0.234$ [22]; the misfit parameter of $In_{0.2}Ga_{0.8}N$ quantum dot in GaN matrix is $\varepsilon^* = 0.021$

The changes of band gaps GaN nanowire depend on the QD misfit parameter $\varepsilon^*$ and shape as shown in Fig. 4. In addition, the band gap depends on the ratio of the sizes of the quantum dot and nanowire.

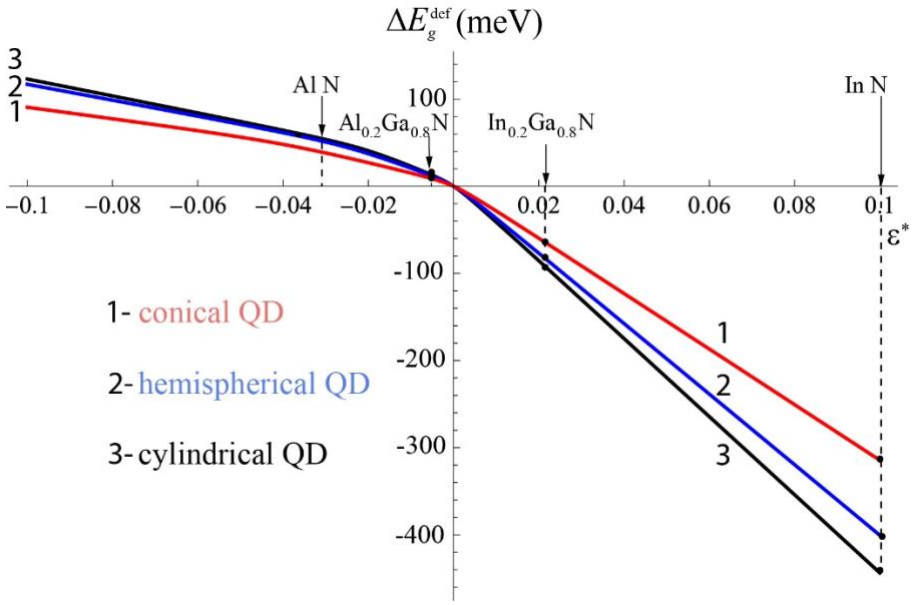


**Fig. 4**. The dependence of maximum band gap change under lateral surface of the GaN nanowire (NW) containing quantum dot (QD) on misfit parameter $\varepsilon^*$. The parameters for calculations: the volume of QD $V = 144\pi$ nm$^3$; the radius of the QD base and NW radius are 6 and 10 nm, respectively; the Poisson ratio $\nu = 0.234$ [22]. The arrows indicate QDs corresponding to the selected misfit parameters

## Discussions and Conclusions

In this study, using the found analytical formulas for the elastic fields of cylindrical, hemispherical, and conical inclusions simulating QDs and located along the semiconductor NW symmetry axis, the maps of the elastic dilations are depicted and the regions of their extremes near the NW free surface are identified. Calculations are performed within the framework of the isotropic linear theory of elasticity. For GaN nanowires containing axisymmetric QDs of varying shapes and compositions, the changes of the band gap in the NW regions of elastic dilation extremes are calculated. The analysis demonstrates that the contribution of the free surface to the elastic fields, as well as the band structure, depend on the QD shape, material and size. The band gap near the free surface of the semiconductor nanowire changes most strongly for a cylindrical QD (Fig. 4). The change of semiconductor NW band gap depends linearly on the positive misfit parameter ($\varepsilon^* > 0$) between QD and NW, for the case of $\varepsilon^* < 0$, the dependence is nonlinear (Fig. 4). It is shown that the band gap of GaN nanowires can locally vary by approximately 10% of the tabulated value.

The response of the band gap of a semiconductor nanowire to the elastic field of a quantum dot embedded in this wire allows one to band gap engineering of the nanowire by varying the shape, material, and size of the quantum dot.

## CRediT authorship contribution statement

**Nguyen Van Tuyen**: data curation; **Anna L. Kolesnikova**: writing – review & editing, writing – original draft; **Mikhail Yu. Gutkin**: conceptualization; **Alexey E. Romanov**: supervision.

## Conflict of interest

The authors declare that they have no conflict of interest.

## References

1. Deshmukh A, Bhaiswar J, Kapse V, Meghe D. Quantum dots: a brief review. In: Thejo Kalyani N, Dhoble SJ, Michalska-domańska M, Vengadaesvaran B, Nagabhushana H, Arof AK (eds.) *Quantum Dots.* Woodhead Publishing; 2023. p.41–66.
2. Efros AL, Brus LE. Nanocrystal quantum dots: From discovery to modern development. *American Chemical Society Nano.* 2021;15(4): 6192–6210.
3. García de Arquer FP, Talapin DV, Klimov VI, Arakawa Y, Bayer M, Sargent EH. Semiconductor quantum dots: Technological progress and future challenges. *Science.* 2021; 373(6555): eaaz8541.
4. Schmidt HM, Weller H. Quantum size effects in semiconductor crystallites: Calculation of the energy spectrum for the confined exciton. *Chemical Physics Letters.* 1986;129(6): 615–618.
5. Park SH, Morgan RA, Hu YZ, Lindberg M, Koch SW, Peyghambarian N. Nonlinear optical properties of quantum-confined CdSe microcrystallites. *Journal of the Optical Society of America B.* 1990;7(10): 2097–2105.
6. Liu Y, Bose S, Fan W. Effect of size and shape on electronic and optical properties of CdSe quantum dots. *Optik.* 2018;155: 242–250.
7. Ngo CY, Yoon SF, Fan WJ, Chua SJ. Effects of size and shape on electronic states of quantum dots. *Physical Review Journals B.* 2006;74(24): 245331.
8. Grundmann M, Stier O, Bimberg D. InAs/GaAs pyramidal quantum dots: Strain distribution, optical phonons, and electronic structure. *Physical Review B.* 1995;52(16): 11969–11981.
9. Pan E, Yang B. Elastic and piezoelectric fields in a substrate AlN due to a buried quantum dot. *Journal of Applied Physics.* 2003;93(5): 2435–2439.
10. Romanov AE, Beltz GE, Fischer WT, Petroff PM, Speck JS. Elastic fields of quantum dots in subsurface layers. *Journal of Applied Physics.* 2001;89(8): 4523–4531.
11. Bir GL, Pikus GE. *Symmetry and Strain-Induced Effects in Semiconductors*. New York: Wiley; 1974.
12. Zhang A, Luo S, Ouyang G, Yang G. Strain-induced optical absorption properties of semiconductor nanocrystals. *Journal of Chemical Physics.* 2013;138(24): 244702.
13. Romanov AE, Baker TJ, Nakamura S, Speck JS. Strain-induced polarization in wurtzite III-nitride semipolar layers. *Journal of Applied Physics.* 2006;100(2): 023522.
14. Chuang SL, Chang CS. K·p method for strained wurtzite semiconductors. *Physical Review B.* 1996;54(4): 2491–2504.
15. Reimer ME, Akopian N, Barkelid M, Bulgarini G, Heeres R, Hocevar M, Witek BJ, Bakkers EPAM, Zwiller V. Single semiconductor quantum dots in nanowires: growth, optics, and devices, in quantum dots. In: Tartakovskii A. (ed.) *Quantum Dots.* Cambridge: Cambridge University Press; 2012. p.21–40.
16. Björk MT, Thelander C, Hansen AE, Jensen LE, Larsson MW, Wellenberg LR, Samuelson L. Few-electron quantum dots in nanowires. *Nano Letters.* 2004;4(9): 1621–1625.
17. Francaviglia L, Fontana Y, i Morral AF. Quantum dots in nanowires. In: Dayeh SA, i Morral AF, Jagadish Ch. (eds.) *Semiconductors and Semimetals.* Elsevier; 2016. p.159–184.
18. Deng J, Yu J, Hao Z, Kang J, Lu B, Wang L, Sun C, Han Y, Xiong B, Wang J, Li H, Luo Y. Disk-shaped GaN quantum dots embedded in AlN nanowires for room-temperature single-photon emitters applicable to quantum information technology. *ACS Applied Nano Materials.* 2022;5(3): 4000–4008.
19. Bouwes Bavinck M, Zieliński M, Witek BJ, Zehender T, Bakkers EPA.M, Zwiller V. Controlling a nanowire quantum dot band gap using a straining dielectric envelope. *Nano Letters.* 2012;12(12): 6206–6211.
20. Kremer PE, Dada AC, Kumar P, Ma Y, Kumar S, Clarke E, Gerardot BD. Strain-tunable quantum dot embedded in a nanowire antenna. *Physical Review B.* 2014;90(20): 201408.

21. Waltereit P, Romanov AE, Speck JS. Electronic properties of GaN induced by a subsurface stressor. *Applied Physics Letters*. 2002;81(25): 4754–4756.
22. Romanov AE, Waltereit P, Speck JS. Buried stressors in nitride semiconductors: Influence on electronic properties. *Journal of Applied Physics*. 2005;97(4): 043708.
23. Denton AR, Ashcroft NW. Vegard's law. *Physical Review A*. 1991;43(6): 3161–3164.
24. Vegard L. Die Konstitution der Mischkristalle und die Raumfüllung der Atome. *Zeitschrift für Physik*. 1921;5(1): 17–26.
25. Kolesnikova AL, Soroka RM, Romanov AE. Defects in the elastic continuum: classification, fields and physical analogies. *Materials Physics and Mechanics*. 2013;17(1): 71–91. (In Russian)
26. Kolesnikova AL, Gutkin MYu, Romanov AE. Analytical elastic models of finite cylindrical and truncated spherical inclusions. *International Journal of Solids and Structures*. 2018;143: 59–72.
27. Nguyen Van Tuyen, Kolesnikova AL, Romanov AE. Isotropic elasticity of dilatational conical inclusion. An analytical approach. *International Journal of Solids and Structure*. 2024;294: 112735.
28. Kolesnikova AL, Nguyen Van Tuyen, Gutkin MYu, Romanov AE. General approach to the calculation of elastic properties of axially symmetric quantum dots in nanowires. *Pisma v Zhurnal Tekhnicheskoi Fiziki*. 2024;50(6): 28–32. (In Russian)
29. Kolesnikova AL, Nguyen Van Tuyen, Gutkin MYu, Romanov AE. Dilatational disk and finite cylindrical inclusion in elastic nanowire. *International Journal of Engineering Science*. 2025;206: 104169.
30. Kolesnikova AL, Romanov AE, Gutkin MYu, Bougrov VE. Multi-step dilatational inclusion in an elastically isotropic cylinder. *Materials Physics and Mechanics*. 2021;47(5): 697–705.
31. Willatzen M, Lew Yan Voon LC. *The k·p Method*. Berlin: Springer; 2009.
32. Chuang SL. *Physics of Optoelectronic Devices*. New York: John Wiley; 1995.
33. Ghosh S, Waltereit P, Brandt O, Grahn HT, Ploog KH. Electronic band structure of wurtzite GaN under biaxial strain in the M plane investigated with photoreflectance spectroscopy. *Physical Review B*. 2002;65(7): 075202.